RAA 2016 Vol. **16** No. **8**, 122 (10pp) doi: 10.1088/1674–4527/16/8/122
http://www.raa-journal.org *http://iopscience.iop.org/raa*

***R**esearch in*
***A**stronomy and*
***A**strophysics*

Large solar energetic particle event that occurred on 2012 March 7 and its VDA analysis

Liu-Guan Ding[1], Xin-Xin Cao[1], Zhi-Wei Wang[1] and Gui-Ming Le[2]

[1] School of Physics and Optoelectronic Engineering, Institute of Space Weather, Nanjing University of Information Science and Technology, Nanjing 210044, China; *dlgedu@163.com*
[2] National Center for Space Weather, China Meteorological Administration, Beijing 100081, China

Received 2016 January 27; accepted 2016 April 11

Abstract On 2012 March 7, the *STEREO Ahead* and *Behind* spacecraft, along with near-Earth spacecraft (e.g. *SOHO*, *Wind*) situated between the two *STEREO* spacecraft, observed an extremely large global solar energetic particle (SEP) event in Solar Cycle 24. Two successive coronal mass ejections (CMEs) have been detected close in time. From the multi-point in-situ observations, it can be found that this SEP event was caused by the first CME, but the second one was not involved. Using velocity dispersion analysis (VDA), we find that for a well magnetically connected point, the energetic protons and electrons are released nearly at the same time. The path lengths to *STEREO-B* (*STB*) for protons and electrons have a distinct difference and deviate remarkably from the nominal Parker spiral path length, which is likely due to the presence of interplanetary magnetic structures situated between the source and *STB*. Also, the VDA method seems to only obtain reasonable results at well-connected locations and the inferred release times of energetic particles in different energy channels are similar. We suggest that good-connection is crucial for obtaining both an accurate release time and path length simultaneously, agreeing with the modeling result of Wang & Qin (2015).

Key words: Sun: particle emission — Sun: coronal mass ejection (CME) — method: velocity dispersion analysis (VDA)

1 INTRODUCTION

Solar energetic particles (SEPs) are charged particles with energies much greater than those of the bulk solar wind, and originate from explosive processes at the Sun such as flares and coronal mass ejections (CMEs), known as "impulsive" events and "gradual" events respectively. Historical studies show that large gradual SEP events are almost always associated with CMEs (Kahler et al. 1984; Reames 1995; Kahler 1996; Gopalswamy et al. 2002; Cliver et al. 2004; Tylka et al. 2003; Kahler & Vourlidas 2013). However, not all fast and wide CMEs lead to large SEP events (Kahler 1996; Ding et al. 2013, 2014a). Kahler (1996); Kahler et al. (2000) noted that although the maximum energy and intensity of energetic particles in large SEP events are generally correlated with CME speed, the scatter is very large, and suggested that the ambient superthermal seed particles can be another important factor for producing large SEP events. The seed population is commonly derived from the materials in solar flares (Mason et al. 1999, 2000; Cane et al. 2006; Ding et al. 2015) and the preceding CMEs (Gopalswamy et al. 2002, 2004; Li et al. 2012; Ding et al. 2013, 2015).

Gopalswamy et al. (2002) first showed that the interaction of two CMEs is an important aspect of SEP production, and the shocks can preferentially accelerate particles from the material of the preceding CMEs rather than from the quiet solar wind. Later, Gopalswamy et al. (2004) found that there is a strong correlation between high particle intensity events and the existence of preceding CMEs within 24 h ahead of the primary CMEs, but there is a poor correlation with the flare class. Then, Li & Ma (2005) proposed that two consecutive CMEs may provide a favorable environment for particle acceleration.

Recently, Ding et al. (2013) suggested that large gradual solar energetic particle events are often associated with twin-CMEs, a scenario first proposed by Li et al. (2012). In this scenario, the preceding CME can provide enough enhanced turbulence and seed population ahead of the main CME-driven shock to generate a more efficient particle acceleration process compared to a single CME (Li et al. 2012; Ding et al. 2015). Based on a statistical analysis of the SEP events in Solar Cycle 23, Ding et al. (2013) found that 61% of twin CMEs lead to large SEP events as compared to only 29% of single fast CMEs leading to large SEP events. However, not all twin-CMEs lead to a large

SEP event (Ding et al. 2013, 2014a), and the relevance of CME-CME interactions for larger SEP events remains unclear (Kahler & Vourlidas 2014).

After the launch of the *STEREO* mission, CME observations from multiple vantage points became available. By using the co-observations of *STEREO* combined with *SOHO* and *SDO*, two CMEs were identified to erupt successively from the same active region (AR) within merely 3 min in the 2012 May 17 ground level enhancement (GLE) event (Shen et al. 2013). Also, Ding et al. (2014b) investigated the eruption and interaction of two CMEs during the large SEP event that occurred on 2013 May 22 using multiple spacecraft observations, and found that the release times of protons and electrons agreed with the time when the second CME caught up with the trailing edge of the first CME, indicating that CME-CME interaction (or shock-CME interaction) played an important role in the process of particle acceleration in that event.

The time at which SEPs are first released into interplanetary (IP) space, and its relation to CMEs and various photon emissions, are important clues to the site and nature of the SEP acceleration mechanism (Lin et al. 1981; Kahler 1994; Tylka et al. 2003; Reames 2009b; Lin 2011). Velocity dispersion analysis (VDA) is an often used tool for obtaining the solar particle release (SPR) time in studying impulsive and gradual SEP events. Plotting onset times versus v^{-1} yields a line with the initial SPR time in the solar vicinity as the intercept and the magnetic path length as the slope. This SPR time only defines the earliest acceleration or release of particles that are unscattered in transit. In this case, SEPs with different energies are assumed to be released at the same time and the same location near the Sun. Using this method, Tylka et al. (2003) examined two impulsive events and three GLEs and found that the SPR times in impulsive events occurred precisely at the peak time of hard X-rays, while those in GLEs often coincided with CME-driven shocks. Reames (2009b) tested all the GLE events in Solar Cycle 23 with the VDA method and found that the path lengths of GLEs vary from 1.1 AU to 2.2 AU and the SPR times in all of the GLEs occur after the onset of the shockwave-induced type II radio emission. Furthermore, Reames (2009a), as well as Gopalswamy et al. (2012), found that acceleration for magnetically well-connected large GLEs begins at $\sim$ 2 solar radii, in contrast to non-GLEs that have been found to be strongly associated with shocks above 3 solar radii. From the VDA analysis, Tan et al. (2013) noted that the deduced path length of low-energy electrons from their release site near the Sun to an observer at 1 AU is consistent with the ion path length deduced by Reames (2009b,a).

However, for many gradual SEP events, the release of particles accelerated to different energies by a CME-driven shock becomes complicated and does not occur at the same time (see e.g. Li et al. 2003, 2005; Ding et al. 2014b). Recently an alternative VDA method was used where the path length of energetic particle was assumed to be the nominal Parker spiral and then utilized to obtain the release times for particles with different energies. Using this method, Kim et al. (2014) suggested a new classification scheme of SEP events based on the release times relative to flares and energy-dependent flux enhancement, unlike the conventional classification of SEP based on whether the flux time profile is impulsive or gradual. In addition, Kim et al. (2015) also implied that there were some different characteristics associated with different groups having different origins and acceleration processes. Following this method (Kim et al. 2014, 2015), Ding et al. (2016) found that there were two particle release processes that occurred in the 2012 May 17 GLE event: the first one is consistent with particles accelerated at the solar flare, and the second one is consistent with particles accelerated at the associated CME-driven shock.

Obviously, the inferred release times and the path lengths have some uncertainties when VDA is applied. Dalla et al. (2003) found that the derived path lengths at Ulysses are 1.06 to 2.45 times the length of a Parker spiral magnetic field line connecting the spacecraft to the Sun, and the time of particle release from the Sun is between 100 and 350 min later than the release time derived from in-ecliptic measurements. To apply the VDA method more reasonably, many studies that performed numerical simulations have been done to investigate the validity of the method. Only when the parallel mean-free paths (MFP) are large enough ($\lambda_{||} > 0.3$ AU) can the IP scattering have an insignificant effect on the derived solar release times (Lintunen & Vainio 2004). Moreover, when the background level is below 0.01 of the peak intensity of the flux, the onset time of the SEP event can be identified precisely (Sáiz et al. 2005). Recently, Wang & Qin (2015) analyzed the accuracy of the VDA method and proposed that an ideal SEP event for VDA analysis should meet the following conditions: impulsive source duration, large parallel MFP, low background level, and good connection between the observer and the source.

To argue whether twin CMEs are the cause of large SEP events, the release time of SEPs at the Sun has to be later than the eruption of the second CME. In principle, one can use the VDA method to obtain the solar release time of SEPs and examine if this is after the eruption of the second CME. However, the VDA methods are subject to uncertainties. Therefore, for twin CMEs erupting closely in time (e.g., within an hour), it is hard to obtain the correct ordering of the SEP release time and the eruption time of the second CME unless accurate VDA can be performed.

In this work, we performed a case study and examined an SEP event where two consecutive CMEs were found. The event occurred on 2012 March 7 and was observed by both *STEREO-A* (*STA*) and *STEREO-B* (*STB*), as well as *Wind* and *ACE*. Applying VDA to multi-spacecraft observations allows us to estimate the SEP release time more accurately than that observed by a single spacecraft. We found that VDA analysis is best applied when the spacecraft is magnetically well-connected to the acceleration site.

2 OBSERVATIONS

We use in-situ and remote-sensing observations from different spacecraft that provide multiple vantage points in this study. The observations included energetic particle fluxes detected from *STEREO*/HET (von Rosenvinge et al. 2008) and similar observations from near-Earth spacecraft (e.g. *SOHO*/ERNE (Torsti et al. 1995; Valtonen et al. 1997) and *Wind*/3DP (Bougeret et al. 1995; Lin et al. 1995)), coronagraph observations from *STEREO*/SECCHI (Howard et al. 2008) and *SOHO*/LASCO (Brueckner et al. 1995), and radio observations from *STEREO*/WAVES (Cecconi et al. 2008) and *Wind*/WAVES.

Figure 1 shows the relative configuration of three spacecraft at 01:00 UT on 2012 March 7. The angular separation between the Earth and *STA* is 109.5°; the angular separation between the Earth and *STB* is 117.8°. Since the associated AR (No. 11429 in NOAA) is located about E20° from the Earth, the event was a backside event for *STA* and a western limb event for *STB*. The propagation direction of two successive CMEs is also marked by the orange arrow.

2.1 CME Observation

On 2012 March 7, an X5.4 flare (onset: 00:02 UT, peak: 00:24 UT, end: 00:40 UT) at E27° was followed by an X1.3 flare (onset: 01:05 UT, peak: 01:14 UT, end: 01:23 UT) at E17°. Two fast halo LASCO CMEs accompanied these events, the first observed above the occulting disk at 00:24 UT (with a speed of 2684 km s^{-1} [1]) and the second at 01:36 UT (1825 km s^{-1}).

Coronagraph observations made by *SOHO*/LASCO, *STA*/COR2 and *STB*/COR2 are shown in Figure 2. Panel a1(c1) is the *STB*(*STA*) COR2 image at 01:39 UT. Panel b1 is the running difference of the *SOHO*/LASCO C3 image (01:39 UT – 01:27 UT). The envelopes of the two CMEs can be clearly seen from these panels. To better examine these two CMEs, we also used the Graduated Cylindrical Shell (GCS, Thernisien et al. (2006, 2009)) model to fit CME1 and CME2. In the bottom panels of Figure 2, the green grids represent the fitting result of CME1 and the red grids represent the fitting result of CME2. From the fitting results, one can see clearly that the propagation directions of these two CMEs have similar longitudes but distinct latitudes in space.

2.2 Radio Bursts

Type II radio bursts are caused by shock-accelerated electrons radiating at local plasma frequencies. As the shock propagates out, the ambient plasma density drops and the radio burst drifts to lower frequencies. Type II radio bursts have been used as a diagnostic of the CME and its driven shock in the corona and IP space in studying SEP events (see e.g. Kahler 1982; Cane et al. 2002; Cliver et al. 2004; Gopalswamy et al. 2005). Figure 3 shows radio observations in the frequency range of 1–14 MHz detected by the WAVES instruments onboard both *STEREO* spacecraft and that on *Wind*. Multiple episodes of type II and type III radio emissions can be seen from the radio dynamic spectra. All three spacecraft observed a bright type III radio burst beginning at about 00:18 UT, which we interpret to be associated with the first flare and coronal eruption. A type II radio burst followed from about 00:35 UT to 01:00 UT. It was not continuous and is marked by white solid lines in each panel. Often both plasma emissions at the fundamental and the second harmonic frequencies can be observed. We believe that this is also the case in this event. The second harmonic branch can be clearly identified in *STB* and *STA*, marked by the white dashed lines in each panel. This type II radio burst is evidently associated with the shock driven by the first CME.

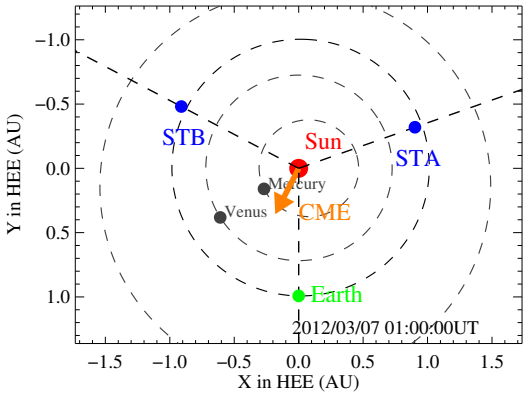

Fig. 1 The positions of the *STA/B* spacecraft and the Earth. The orange arrow indicates the propagation direction of the associated CME.

Later, the second type III radio burst was detected from about 01:09 UT to 01:30 UT. It is associated with the second flare eruption. There are also other type II radio burst episodes shown between 01:38 UT and 02:05 UT. From the radio spectra of the *Wind*/WAVES shown in panel (b), we can clearly see the fundamental and second harmonic branches. These are clearly not the continuations of those type II radio emissions associated with the first CME. So, we interpret the second type II radio bursts to be associated with the shock driven by the second CME in this event. From the start frequency of these two episodes of type II radio bursts, we see that the first shock is formed at lower height than the second one.

2.3 In-Situ Observation of SEPs

Figure 4 shows one-minute averaged energetic proton observations from the *STB*(*STA*)/HET and *SOHO* ERNE/HED respectively in panels (a), (b) and (c) during the onset of this SEP event. The shaded areas indicate the ascending period in each in-situ observation. As shown in the figure, the event was a global event and seen in all three

[1] *http://cdaw.gsfc.nasa.gov/CME_list/UNIVERSAL/2012_03/univ2012_03.html*

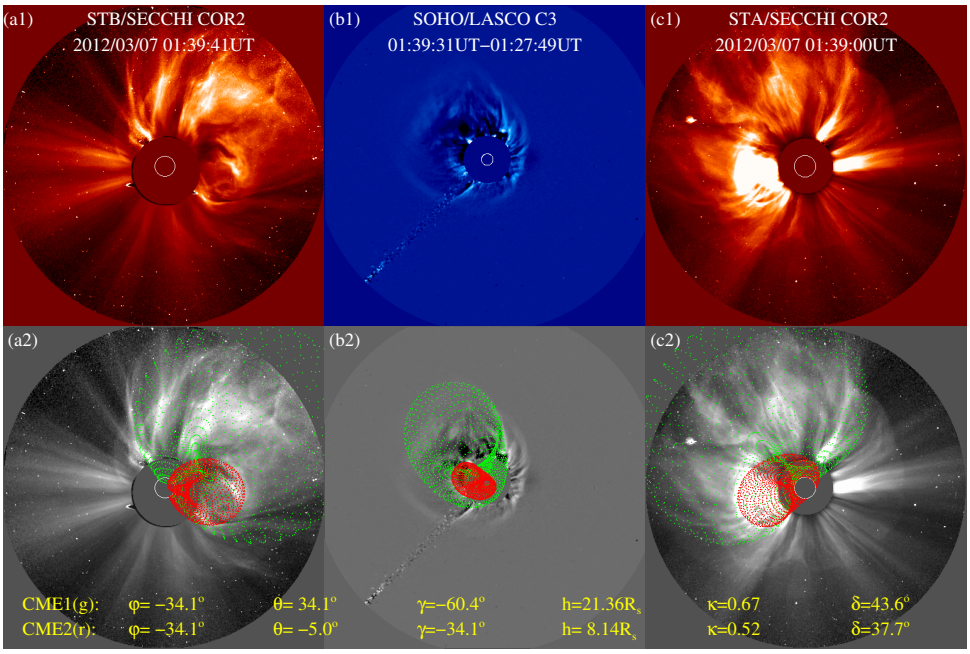

Fig. 2 The two CMEs during this SEP event detected by *STA*(/*B*)/SECCHI and *SOHO*/LASCO (*top panels*), and their GCS model fitting results (*bottom panels*).

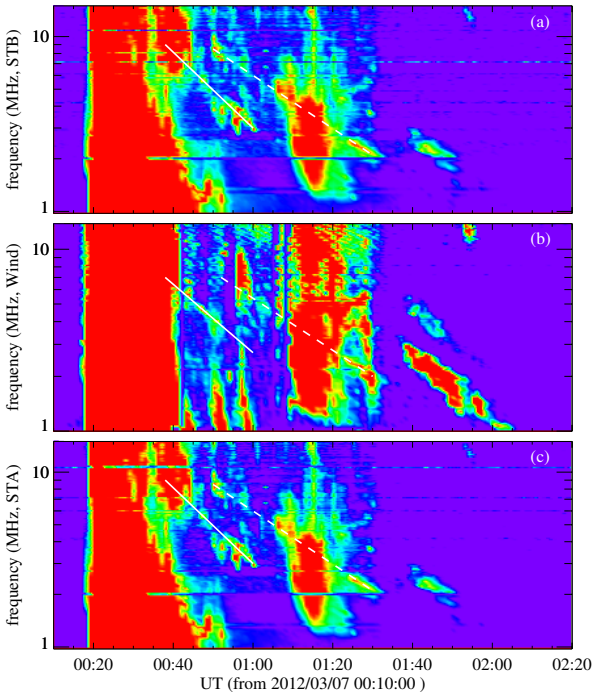

Fig. 3 The radio burst observations detected by three spacecraft (*STA*(*B*)/WAVES and *Wind*/WAVES). The white lines in each panel show the shift of type II radio bursts. The solid lines mark the fundamental branch, and the dashed lines mark the second harmonic branch.

spacecraft. The HET instrument onboard *STB* was best magnetically connected. It detected prompt enhancements in all energy channels from ∼01:15 UT to ∼02:10 UT on March 7, with clear velocity dispersion. These onset times are delayed by about 40 min (due to propagation) from the release near the Sun (see Sect. 3). These SEPs are clearly consistent with the first solar eruption before 01:00 UT but are inconsistent with the second solar eruption after 01:00 UT. Then *SOHO* detected gradual enhancements in all energy channels within 4.5 hours after about 02:10 UT. The peak flux intensity in *SOHO* was ∼ 10 times lower than that observed in *STB*. Later, *STA* also detected gradual

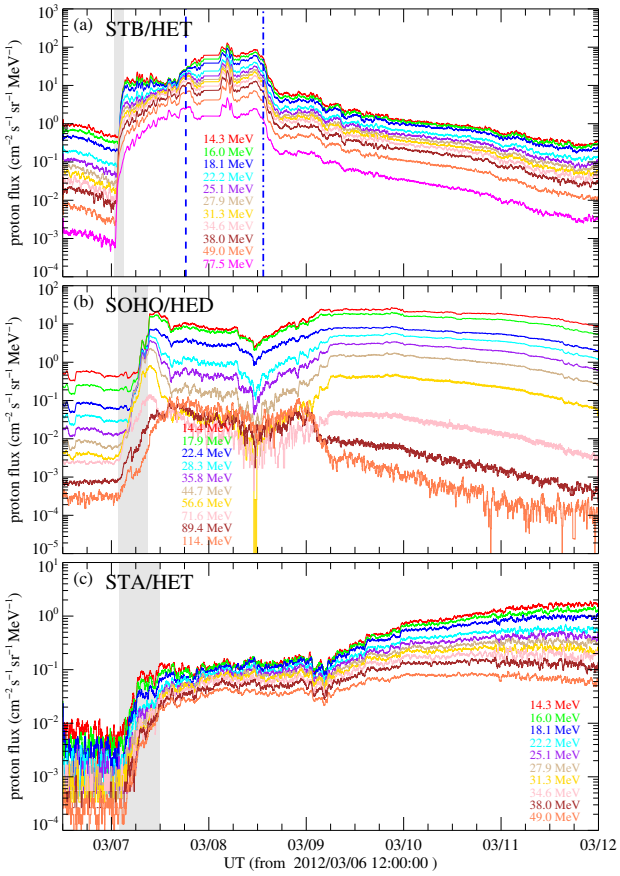

Fig. 4 The solar energetic protons detected by three spacecraft (*STA/B* and *SOHO*/ERNE). The shaded areas identify the interval of energetic proton enhancement in each observation. The vertical dashed line and dot-dashed line in panel (a) indicate the time of IP shocks corresponding to the solar wind observations shown in Fig. 6.

enhancement in all energy channels within about 3 hours, and the peak intensity was also ∼10 times lower than that observed in *SOHO*. The onsets in *SOHO* and *STA* were after the second CME. Therefore from only the *SOHO* and *STA* observation, one cannot tell if the in-situ SEPs are due to the shock driven by the 1st CME or the 2nd CME.

However, with *STB* observation, which is well magnetically situated, we can clearly identify that these SEPs are accelerated by the 1st CME-driven shock. We note that the first shock was formed at a lower height, which is more suitable for leading to a high intensity SEP event or GLE event (Reames 2009a; Gopalswamy et al. 2012; Mewaldt et al. 2012).

Our study shows that multi-vantage-point observations are crucial in understanding SEP events.

We next examine the observations of energetic electrons from multi-vantage points in Figure 5. From panel (a) of this figure, the electron intensity at *STB*/SEPT clearly increased rapidly in all energy channels by ∼00:50 UT. About 30 min later, the *STA* detected gradual enhancements in all energy channels, as shown in panel (c). Unexpectedly, the energetic electron flux detected by *Wind*/3DP seemed to start to increase very gradually at about 00:00 UT as displayed in panel (b). Due to the passage of an IP shock recorded by the *Wind* spacecraft at about 03:30 UT on March 7, which may cause a slow rise beginning several hours before the shock (Tsurutani & Lin 1985), the time profiles from that time are contaminated and it is difficult to accurately identify their onsets. Again, only *STB*, the best-connected detector, provides unambiguous association between the energetic electrons and the first CME-driven shock. Neither *STA* nor *SOHO* can reveal this association.

2.4 In-Situ Observation of Solar Wind

The intensity time profile of solar wind detected by *STB* became more complicated by the passage of shocks, sheaths and IP coronal mass ejections (ICMEs) on March 7–8. In particular, the intensities weakly increased at about 18:20 UT on March 7 and sharply decreased at about 13:25 UT on March 8, which were probably associated with the passage of two ICMEs and/or their corresponding shocks as shown in Figure 6. Increases of SEP intensities observed in association with the passage of transient IP shocks are known as energetic storm particle events (Bryant et al. 1962; Reames 1999). There are also cases where there are decreases in the time profiles associated

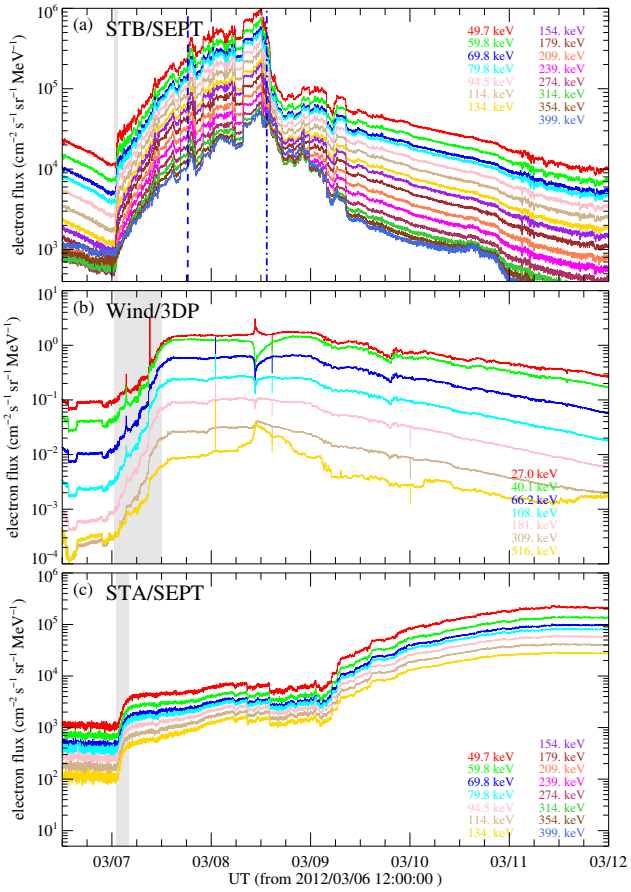

Fig. 5 The in-situ observations of solar energetic electrons detected by three spacecraft (*STA/B* and *Wind*/3DP). The shaded areas identify the intervals of energetic electron enhancement in each observation. The vertical lines in panel (a) show the time of IP shocks, in the same way as those in Fig. 4(a).

with shock passage. For example, Hietala et al. (2011) noted that such decreases may occur due to an accelerated particle trapped between shocks (e.g. see the *Wind* observations at the second shock passage in Hietala et al. (2011)). The first shock (denoted by vertical dashed lines) followed by a hypothetical ICME structure was detected at about 18:20 UT, which erupted on March 5 from AR 11429. Because this ICME is situated between the source and *STB* when the accelerated particles start to escape in the solar vicinity, the propagation path length of particles observed by *STB* presents a distinguishable difference from the nominal Parker spiral path length corresponding to solar wind speed (see VDA results below). The second shock (denoted by vertical dot-dashed lines) followed by an ICME detected at about 13:25 UT on March 8 was probably produced by the first CME launched at 00:24 UT on March 7 mentioned before. This shock can also be observed by the spacecraft near the Earth (not shown here). For energetic protons and electrons, the intensities in *STB* and *SOHO* present a nominal decay phase after the passage of the shock, while those in *STA* show a second enhancement in this period (after ∼05:00 UT on March 9). It is very interesting to find that there is a corotating interaction region (CIR) passing through the *STA* coincidentally at that time, which may be considered to contribute to the second enhancement, as the CIR is also an efficient particle accelerator (Fisk & Lee 1980; Reames et al. 1997; Zhao et al. 2016).

3 VELOCITY DISPERSION ANALYSIS

To compare the solar energetic particle releases with those of other associated solar activities, it is necessary to compensate proton travel time from the Sun corresponding to their energies. We apply VDA to the proton data obtained from *STEREO*/HET and *SOHO* ERNE/HED, and the electron data obtained from *STEREO*/SEPT and *Wind*/3DP. To obtain the solar release time, we use

$$t_{\rm onset} = t_{\rm rel} + t_{\rm trans} = t_{\rm rel} + L/v(E) \qquad (1)$$

where $t_{\rm rel}$ is the particle release time at its source region near the Sun; $t_{\rm trans} = L/v(E)$ is the travel time for a particle with energy E; L is the propagation path length and $v(E)$ is the velocity of an energetic particle with energy E. We determined the onset times by following the procedure outlined in Ding et al. (2014b, 2016). The onset time is decided by $f(t_{\rm onset}) = \langle f \rangle + 2\sigma$, where $\langle f \rangle$ is the average of the pre-event background and σ is its standard deviation.

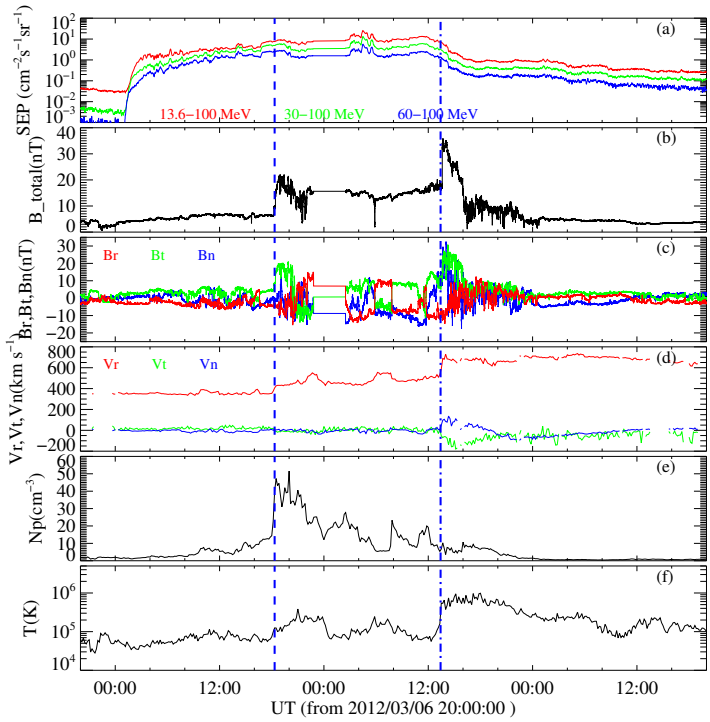

Fig. 6 The solar wind observations recorded from the location of *STB*. The vertical dashed lines and dot-dashed lines in each panel represent two IP shocks.

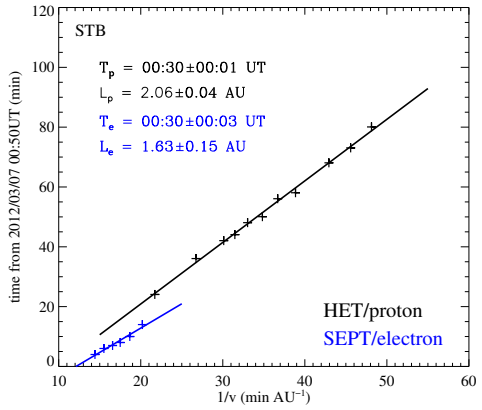

Fig. 7 The VDA of energetic protons (black line with crosses) and energetic electrons in low energy channels (blue line with crosses) detected by *STB*.

So, the onset time signals the time when the distribution function f becomes 2σ higher than the background. The uncertainty of the onset time mainly comes from possible measurement uncertainty, such as data resolution. We also calculate a possible uncertainty by using either 3σ or 1σ (e.g. see Ding et al. 2016).

For data on energetic protons and electrons obtained from *STEREO* and near Earth spacecraft (*SOHO* and *Wind*), we first applied VDA assuming all first arriving energetic particles are released at the same time from their source and propagate scatter free along the IP magnetic field lines. It is hard to address the uncertainty due to the scatter-free assumption, because the pitch angles of the first arriving energetic particles cannot be determined exactly along the transport path from the Sun to the observer. However, if we use Equation (1), a nonzero pitch angle would result in the experimental path length being larger than the actual path length by approximately a factor of $1/\cos\theta$, with θ representing the pitch angle of the first arriving particles, and estimates of the release time are accurate to the order of several minutes for the first method used for VDA (Dalla et al. 2003; Sáiz et al. 2005).

Unfortunately, except for *STB* (the best-connected spacecraft), all other observations show poor velocity dispersion and the inferred VDA results are unreliable. Here, we only display the results of the *STB* observations. As shown in Figure 7, the $t_{\rm onset}$s are plotted as a function of $1/v$ for energetic protons and electrons. The black cross symbols represent the protons in all energy channels observed by HET and the blue cross symbols signify the electrons in low energy channels observed by SEPT. It is obviously indicated that the velocity dispersion distribution of the protons does not overlap with that of the electrons. We fitted the points of energetic protons and electrons separately. From the fitting results, it is interesting to find that the protons and electrons were released at the same time, ∼00:30 UT, but they have different propagation path lengths. The path length of protons is ~ 2.06 AU, and that of electrons is ~ 1.63 AU, while the nominal Parker

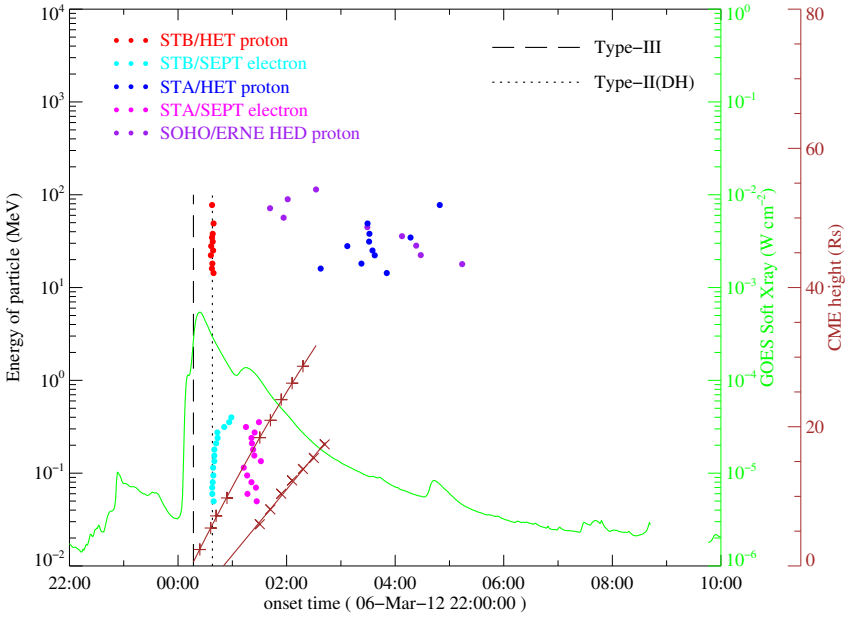

Fig. 8 SPR times near the Sun of SEPs detected by different spacecraft in different energies and related eruptive phenomena including flares, CMEs and radio bursts. The green line shows the soft X-rays detected by *GOES* in $1-8$ Å. The brown lines with different symbols display the heliocentric heights of the first CME (with '$+$' symbols) and second CME (with '$\times$' symbols) as a function of time.

spiral length from the Sun to *STB* with a solar wind speed of 353 km s^{-1} is $\sim$ 1.25 AU. This path length of energetic particles may be caused by the presence of the ICME structure situated between the source region and the detector. Such a structure may also be the reason that the path length of protons is distinct from that of electrons.

In order to reveal the release process of energetic particles at different longitudes, the release times in all energy channels derived from the data acquired by different detectors are shown in Figure 8. Here we assume that the particles with different energies are transported along the nominal Parker spiral if there is no special magnetic structure situated between the Sun and the detector. To compare with, e.g., CME eruption and radio observations, we add 8.3 min, the travel time of light from the Sun to the Earth, to the release time $t_{\rm rel}$. For the energetic protons observed by *STB*, we use the deduced path length of 2.06 AU obtained above as their actual transport path length, as well as 1.63 AU as that of energetic electrons. Under the assumption of scatter free propagation, the release times of protons and electrons in different energy channels are obtained, as indicated by the red points and cyan points in the figure respectively. From the distribution of the release times versus particle energies, it is clear that all protons and electrons (except from high energy channels) observed by *STB* were released at about the same time. This time also coincided with the start time of DH type II radio bursts (signified by the vertical dotted line) that are associated with the first CME driven shock. The simultaneity of the particle release in all energy channels for protons and low energy electrons supports the proposal that the IP magnetic field in this event was distorted by some IP structures and that the path lengths for electrons and protons are different. It also suggests that the result from VDA as shown in Figure 7 is reliable.

As a comparison, we also calculate the release times of energetic particles detected by *STA* and *SOHO* using the VDA method. We assume a nominal Parker spiral path length (1.16 AU for *STA* and 1.18 AU for *SOHO*) as no considerable IP magnetic structures were between the Sun and *STA* and *SOHO*. From the figure, one can see that the release times of protons with different energies as observed by *SOHO* and *STA* have large scatters. This implies that energetic protons in different energy channels may not be released at the same time or that they have propagated along different paths. It should be noted that *SOHO* and *STA* were not well-connected with the source region in this event. So, if we apply the VDA to *SOHO* or *STA* in this event (the results are not shown here), one can find that it does not yield a fine result of release time or path length like *STB*.

Since the particle release times for *STA* and *SOHO* show large scatters, these release times cannot be used to compare with other solar activities. This is because both *STA* and *SOHO* are poorly-connected spacecraft. Indeed, if one were to use the releases of protons observed by *SOHO* and *STA*, one may mistakenly arrive at the conclusion that these SEPs are associated with the shock driven by the second CME.

As shown in the figure, the energetic electrons detected by *STA*/SEPT seem to be released at almost the same time but with slight scatter. We also apply the VDA to these data to obtain the electron release time and path length. It

is interesting that the calculated path length is similar to the nominal Parker spiral path length. The resultant release time is about 01:13 UT, which coincided with the peak time of the second flare, but the uncertainty of the result is large ($\pm$9 min). Note that the protons and electrons observed by *STA* yield different release times.

From our event, we see that one should be very cautious when using VDA to obtain the path length and SEP release time. Under the assumption that particles are released at the same time from the solar vicinity in different energy channels, it seems that a reasonable transport path length from the Sun to the observer can be obtained, even if there are magnetic structures situated between the source and detector. However, the release times may be different for different observers located at different longitudes, suggesting that the release time can strongly depend on whether the spacecraft is well magnetically connected or not. This is realistic since the acceleration site can be connected to different field lines at different times. Usually, the energetic particles are released later when the foot point of the observer is far away from the source region, because of the shock expansion along the longitude during the propagation outward. Alternatively, energetic particles may undergo cross-field diffusion. Finally, we note that there can exist significant differences between ions and electrons in both the release time and the path length.

4 CONCLUSIONS AND DISCUSSION

In this paper, we performed a case study of the SEP event that occurred on 2012 March 7 using in-situ and remote-sensing observations of different spacecraft, offering multi-vantage observations. There were two X-class solar flares and fast and wide successive CMEs erupting from the same source region during the event. These two CMEs agree with the proposed twin-CME scenario (Li et al. 2012; Ding et al. 2013, 2014b), except that in this event the second CME was slower than the first one. Analyses of particle onset and release indicate that particle acceleration in this event was associated with the first solar event/CME and that the second CME was not involved, in agreement with the result of Richardson et al. (2014). In addition, there is no obvious indication in the *STB* intensity time profile of a second particle injection that was associated with the second solar event. Energetic particles that are accelerated at the second CME-driven shock, as suggested by the twin-CMEs scenario (Li et al. 2012), may not be in operation in this event.

The release time of the protons and electrons detected by the best-connected *STB* coincided well with the start time of the type II (DH) radio bursts associated with the first CME shock, which occurred after the peak time of the first flare but prior to that of the second flare. This means both energetic protons and electrons in this SEP event were accelerated only by the first CME-driven shock. On the contrary, if we only consider the release time deduced from observations by single spacecraft that are not well-connected (e.g. *SOHO* or *STA* in this event) via the VDA method, then, for either protons or electrons, we will mistakenly conclude that the second solar eruption is responsible for this SEP event.

When applying the VDA analysis and in particular examining data from multiple spacecraft, we note that certain issues need to be carefully considered. These are as follows.

(1) In the first VDA method that is mentioned in Section 1, the assumption of all particles being released at the same time is usually not satisfied (see four classes in Kim et al. 2014), because the particle acceleration process is different from event to event. Even in a single event, this condition may not be met in different longitudes, especially for not-well-connected points, such as the cases of *SOHO* and *STA* observations in this event.
(2) If some magnetic structures (e.g. ICME) lie between the detector and source region, the path length may have a large difference from the nominal Parker spiral path length, such as the results of the *STB* in this event. The path length of protons and electrons may also differ.
(3) If particles are not released at the same time, one can use the second VDA method mentioned above and examine the associations and acceleration process of one SEP event (Kim et al. 2014). Under such cases, the assumption of the path length being that from the nominal Parker spiral is often made. However, this is only appropriate if there is no large magnetic structure in IP space. For observations made at not-well-connected vantage points, caution must also be exercised because time intensity profiles made at these locations may not yield clear onset times.

As a result, we suggested that to accurately estimate a reasonable release time and path length for energetic particles via the VDA method, VDA should be performed using data from a well-connected spacecraft. This conclusion agrees with the modeling result of Wang & Qin (2015). Furthermore, the standard assumption of a scatter-free IP space needs to be made. Under these conditions, the VDA method can be applied in two different cases: in the first, one can use VDA assuming particles with different energies are released at the same time; this practice is often done when we are almost certain that the IP fields are not Parker-like (e.g. a pre-existing magnetic cloud structure between the Sun and the spacecraft); in the second, one often adopts a nominal Parker field and then the VDA can be used to obtain the release times for particles with different energies.

Acknowledgements We are grateful to the *STEREO*, *SOHO* and *Wind* projects, and the CDAW database for making their data available online. This work is supported at NUIST by the National Natural Science Foundation of China (NSFC)-41304150 for Ding L.G.; at CMA by NSFC-41274193 and 41474166 for Le G.M.

References

Bougeret, J.-L., Kaiser, M. L., Kellogg, P. J., et al. 1995, Space Sci. Rev., 71, 231

Brueckner, G. E., Howard, R. A., Koomen, M. J., et al. 1995, Sol. Phys., 162, 357

Bryant, D. A., Cline, T. L., Desai, U. D., & McDonald, F. B. 1962, J. Geophys. Res., 67, 4983

Cane, H. V., Erickson, W. C., & Prestage, N. P. 2002, Journal of Geophysical Research (Space Physics), 107, 1315

Cane, H. V., Mewaldt, R. A., Cohen, C. M. S., & von Rosenvinge, T. T. 2006, Journal of Geophysical Research (Space Physics), 111, A06S90

Cecconi, B., Bonnin, X., Hoang, S., et al. 2008, Space Sci. Rev., 136, 549

Cliver, E. W., Kahler, S. W., & Reames, D. V. 2004, ApJ, 605, 902

Dalla, S., Balogh, A., Krucker, S., et al. 2003, Annales Geophysicae, 21, 1367

Ding, L., Jiang, Y., Zhao, L., & Li, G. 2013, ApJ, 763, 30

Ding, L.-G., Li, G., Dong, L.-H., et al. 2014a, Journal of Geophysical Research (Space Physics), 119, 1463

Ding, L.-G., Li, G., Jiang, Y., et al. 2014b, ApJ, 793, L35

Ding, L.-G., Li, G., Le, G.-M., Gu, B., & Cao, X.-X. 2015, ApJ, 812, 171

Ding, L.-G., Jiang, Y., & Li, G. 2016, ApJ, 818, 169

Fisk, L. A., & Lee, M. A. 1980, The Astrophysical Journal, 237, 620

Gopalswamy, N., Yashiro, S., Michałek, G., et al. 2002, ApJ, 572, L103

Gopalswamy, N., Yashiro, S., Krucker, S., Stenborg, G., & Howard, R. A. 2004, Journal of Geophysical Research (Space Physics), 109, A12105

Gopalswamy, N., Aguilar-Rodriguez, E., Yashiro, S., et al. 2005, Journal of Geophysical Research (Space Physics), 110, A12S07

Gopalswamy, N., Xie, H., Yashiro, S., et al. 2012, Space Sci. Rev., 171, 23

Hietala, H., Agueda, N., AndréEová, K., et al. 2011, Journal of Geophysical Research (Space Physics), 116, A10105

Howard, R. A., Moses, J. D., Vourlidas, A., et al. 2008, Space Sci. Rev., 136, 67

Kahler, S. 1994, ApJ, 428, 837

Kahler, S. W. 1982, ApJ, 261, 710

Kahler, S. W. 1996, in American Institute of Physics Conference Series, 374, eds. R. Ramaty, N. Mandzhavidze, & X.-M. Hua, 61

Kahler, S. W., Reames, D. V., & Burkepile, J. T. 2000, in Astronomical Society of the Pacific Conference Series, 206, High Energy Solar Physics Workshop - Anticipating HESSI, eds. R. Ramaty & N. Mandzhavidze, 468

Kahler, S. W., Sheeley, Jr., N. R., Howard, R. A., et al. 1984, J. Geophys. Res., 89, 9683

Kahler, S. W., & Vourlidas, A. 2013, ApJ, 769, 143

Kahler, S. W., & Vourlidas, A. 2014, ApJ, 791, 4

Kim, R.-S., Cho, K.-S., Lee, J., et al. 2015, Journal of Geophysical Research (Space Physics), 120, 7083

Kim, R.-S., Cho, K.-S., Lee, J., Bong, S.-C., & Park, Y.-D. 2014, Journal of Geophysical Research (Space Physics), 119, 9419

Li, G., Moore, R., Mewaldt, R. A., Zhao, L., & Labrador, A. W. 2012, Space Sci. Rev., 171, 141

Li, G., Zank, G. P., & Rice, W. K. M. 2003, Journal of Geophysical Research (Space Physics), 108, 1082

Li, G., Zank, G. P., & Rice, W. K. M. 2005, Journal of Geophysical Research (Space Physics), 110, A06104

Li, Y.-F., & Ma, J. X. 2005, in American Institute of Physics Conference Series, 799, New Vistas in Dusty Plasmas, eds. L. Boufendi, M. Mikikian, & P. K. Shukla, 173

Lin, R. P. 2011, Space Sci. Rev., 159, 421

Lin, R. P., Potter, D. W., Gurnett, D. A., & Scarf, F. L. 1981, ApJ, 251, 364

Lin, R. P., Anderson, K. A., Ashford, S., et al. 1995, Space Sci. Rev., 71, 125

Lintunen, J., & Vainio, R. 2004, A&A, 420, 343

Mason, G. M., Dwyer, J. R., & Mazur, J. E. 2000, ApJ, 545, L157

Mason, G. M., Mazur, J. E., & Dwyer, J. R. 1999, ApJ, 525, L133

Mewaldt, R. A., Looper, M. D., Cohen, C. M. S., et al. 2012, Space Sci. Rev., 171, 97

Reames, D. V. 1995, Reviews of Geophysics Supplement, 33, 585

Reames, D. V., Ng, C. K., Mason, G. M., et al. 1997, Geophys. Res. Lett., 24, 2917

Reames, D. V. 1999, Space Sci. Rev., 90, 413

Reames, D. V. 2009a, ApJ, 706, 844

Reames, D. V. 2009b, ApJ, 693, 812

Richardson, I. G., von Rosenvinge, T. T., Cane, H. V., et al. 2014, Sol. Phys., 289, 3059

Sáiz, A., Evenson, P., Ruffolo, D., & Bieber, J. W. 2005, ApJ, 626, 1131

Shen, C., Li, G., Kong, X., et al. 2013, ApJ, 763, 114

Tan, L. C., Malandraki, O. E., Reames, D. V., et al. 2013, ApJ, 768, 68

Thernisien, A. F. R., Howard, R. A., & Vourlidas, A. 2006, ApJ, 652, 763

Thernisien, A., Vourlidas, A., & Howard, R. A. 2009, Sol. Phys., 256, 111

Torsti, J., Valtonen, E., Lumme, M., et al. 1995, Sol. Phys., 162, 505

Tsurutani, B. T., & Lin, R. P. 1985, J. Geophys. Res., 90, 1

Tylka, A. J., Cohen, C. M. S., Dietrich, W. F., et al. 2003, International Cosmic Ray Conference, 6, 3305

Valtonen, E., Peltonen, J., Peltonen, P., et al. 1997, Nuclear Instruments and Methods in Physics Research A, 391, 249

von Rosenvinge, T. T., Reames, D. V., Baker, R., et al. 2008, Space Sci. Rev., 136, 391

Wang, Y., & Qin, G. 2015, ApJ, 799, 111

Zhao, L., Li, G., Ebert, R. W., et al. 2016, Journal of Geophysical Research (Space Physics), 121, 77